



Comparative analyses of secreted proteins from the phytopathogenic fungus *Verticillium dahliae* in response to nitrogen starvation

Jun Chu^a, Wei-Fang Li^a, Wang Cheng^a, Mo Lu^a, Ke-Hai Zhou^b, He-Qin Zhu^b, Fu-Guang Li^{b,*}, Cong-Zhao Zhou^{a,**}

^a School of Life Sciences, University of Science and Technology of China, Hefei, Anhui 230027, People's Republic of China

^b State Key Laboratory of Cotton Biology, Institute of Cotton Research, Chinese Academy of Agriculture Sciences (CAAS), Anyang, Henan 455000, People's Republic of China

ARTICLE INFO

Article history:

Received 16 October 2014

Received in revised form 6 February 2015

Accepted 9 February 2015

Available online 16 February 2015

Keywords:

Pathogenic fungi
Verticillium dahliae
Secreted proteins
Nitrogen starvation
Mass spectrometry

ABSTRACT

The soilborne fungus *Verticillium dahliae* is the major pathogen that causes the verticillium wilt disease of plants, which leads to huge economic loss worldwide. At the early stage of infection, growth of the pathogen is subject to the nutrition stress of limited nitrogen. To investigate the secreted pathogenic proteins that play indispensable roles during invasion at this stage, we compared the profiles of secreted proteins of *V. dahliae* under nitrogen starvation and normal conditions by using in-gel and in-solution digestion combined with liquid chromatography–nano-electrospray ionization tandem mass spectrometry (LC–nanoESI-MS). In total, we identified 212 proteins from the supernatant of liquid medium, including 109 putative secreted proteins. Comparative analysis indicated that the expression of 76 proteins was induced, whereas that of 9 proteins was suppressed under nitrogen starvation. Notably, 24 proteins are constitutively expressed. Further bioinformatic exploration enabled us to classify the stress-induced proteins into seven functional groups: cell wall degradation (10.5%), reactive oxygen species (ROS) scavenging and stress response (11.8%), lipid effectors (5.3%), protein metabolism (21.1%), carbohydrate metabolism (15.8%), electron–proton transport and energy metabolism (14.5%), and other (21.0%). In addition, most stress-suppressed proteins are involved in the cell-wall remodeling. Taken together, our analyses provide insights into the pathogenesis of *V. dahliae* and might give hints for the development of novel strategy against the verticillium wilt disease.

© 2015 Elsevier B.V. All rights reserved.

1. Introduction

The infection of the soilborne phytopathogenic fungi *Verticillium dahliae* leads to the vascular wilt disease of cotton and the other crops, resulting in almost complete yield loss [1,2]. During the invasion, the fungi secrete a variety of proteins into the host plant to facilitate the pathogenicity and colonization, and/or produce microsclerotia for the survival in the soil for decades, making it extremely difficult to control the vascular wilt [3–5]. However, it remains unclear how the wilt disease is triggered by the virulence proteins secreted from the pathogen.

At the early stage of infection, the pathogens are subject to the stress of nitrogen starvation [6–8]. Moreover, it was reported that the secreted products of *Magnaporthe grisea* under nitrogen starvation–stress are able to induce the disease symptom expression during rice blast infections [9]. Several bacterial and fungal genes have been found to be specifically induced during nitrogen starvation and/or during infection to the host [6,9–11]. These observations indicated that the stress at the stage of fungal invasion could be simulated by nitrogen starvation.

Thus, the analysis of secreted proteins in response to nitrogen starvation can provide us a better understanding of the fungal pathogenesis, especially at the early stage of invasion.

As an efficient tool, proteomic analysis has been applied to systematically identify pathogenesis-related proteins from the pathogenic fungi, such as *Aspergillus niger*, *Aspergillus flavus*, *Botrytis cinerea*, *Fusarium graminearum* and *Ustilago maydis* [12–17]. A proteomic analysis of *Magnaporthe oryzae* responsive to nitrogen starvation has recently identified 89 differentially produced proteins [18]. Moreover, a comparative proteomic analysis of the highly and weakly aggressive *V. dahliae* isolates identified eighteen unique proteins, which were proposed to play important roles in infecting the host and for the survival of fungi in the soil [19]. However, it remains unknown how the secretome of *V. dahliae* contributes to the invasion into the plant host.

To address this question, we extracted the secreted proteins of *V. dahliae* under the nitrogen starvation, and analyzed the secretome using the liquid chromatography–nano-electrospray ionization tandem mass spectrometry (LC–nanoESI-MS) combined with in-gel or in-solution digestion. A total of 109 secreted proteins were identified, including 76 proteins induced whereas 9 suppressed, suggesting early production of prerequisite proteins for successful infection of the host. Furthermore, we firstly detected 17 unreported proteins here. All these

* Corresponding author. Tel./fax: +86 372 2525381.

** Corresponding author. Tel.: +86 551 63600406.

E-mail addresses: lifug@cricaas.com.cn (F.-G. Li), zczz@ustc.edu.cn (C.-Z. Zhou).

bioinformatic analysis results could improve our understanding of the secretory mechanisms of *V. dahliae* and its early invasive growth in host cell.

2. Materials and methods

2.1. Growth assessments of *V. dahliae* isolates

The single-spore isolates of *V. dahliae* Vd07038 were collected from the infected plant tissues in Anyang cotton experimental fields, Henan Province, China. The fungi were cultured in Czapek-Dox broth (CDB) liquid medium (NaNO₃ 2.0 g/L, K₂HPO₄ 1 g/L, KCl 0.5 g/L, MgSO₄ 0.5 g/L, FeSO₄ 0.01 g/L and sucrose 30 g/L) at 25 °C by shaking at 150 rpm. For each flask, one 0.9 mm-diameter plug was chosen from the edge of the growing culture and transferred into 400 mL of autoclaved CDB liquid medium. Fungal growth was evaluated with the dry weight of the fungal biomass per day in the successive ten days. The averages of three replicates for dry weight of the fungal biomass were recorded.

After incubation for seven days under the normal condition, the fungi were collected. After three times wash with ice-cold sterilized water, the cell pellet was transferred to CDB liquid medium without nitrogen (K₂HPO₄ 1.0 g/L, KCl 0.5 g/L, MgSO₄ 0.5 g/L, FeSO₄ 0.01 g/L, sucrose 30 g/L). Meantime dry weight of the fungal biomass was evaluated at every 12 h over 120 h, respectively.

2.2. Extraction of secreted proteins

The culture supernatant were centrifuged at 12 000 g and filtrated to discard the cell, then added with trichloroacetic acid (TCA) at a final concentration of 10% (w/v) on ice for 30 min. After centrifugation at 10,000 g, 4 °C for 30 min, the pellets were collected and washed with ice-cold 100% (v/v) acetone to remove TCA. After centrifugation at 10 000 g, 4 °C for 30 min, the pellets were collected and dried. To measure the protein concentration, pellets were dissolved in 100 mM Tris-HCl, pH 8.0 and then applied to the BCA protein assay kit (Thermo Scientific). To prepare the samples for electrophoresis, protein pellets were dissolved in SDS-PAGE buffer (250 mM Tris-HCl, pH 8.8, 0.2% (w/v) bromophenol blue, 4% (w/v) SDS, 20% glycerol, 100 mM β-thioglycol) and incubated at 95 °C for 10 min.

2.3. Gradient SDS-PAGE, in-gel and in-solution digestions

The resuspended protein mixture from Vd07038 was first separated through the gradient SDS-PAGE. Briefly, 0.8–1.0 g of dry biomass corresponding culture supernatant was used for secreted protein extraction. Acrylamide gradient was between 8% and 15% [20]. After the electrophoresis, the gel was stained with silver staining [21], showing the presence of proteins with different molecular weights from 14 kDa to 120 kDa. The gel was firstly manually cut into 8 dark stained slices depending on protein molecular weight (MW), and the other light stained

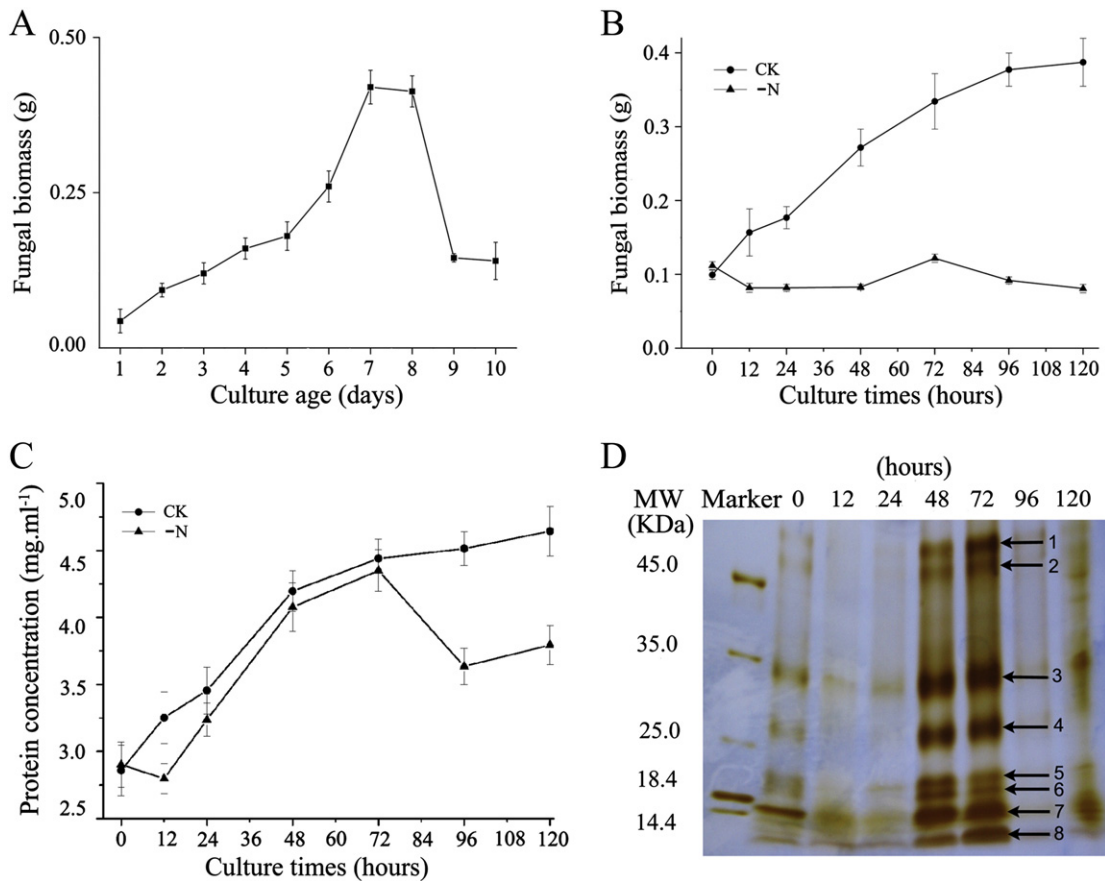


Fig. 1. The growth curve and the profile of secreted proteins of *V. dahliae*. (A) Fungal biomass of *V. dahliae* Vd07038 under normal condition (CDB liquid medium). (B) Fungal biomass of *V. dahliae* and (C) the secreted protein amounts at different time points under normal and nitrogen starvation condition. The fungi after 7-day normal culture were transferred to the nitrogen starvation condition (CDB liquid medium without nitrogen), whereas CK was under the fresh normal condition. Each data point represents an average of three independent biological replicates ± standard error. (D) The gradient SDS-PAGE of secreted proteins of *V. dahliae* Vd07038 under nitrogen starvation condition. Acrylamide concentration of gradient gel was prepared from 8% to 15%. The gel was stained with silver staining. Numbers indicate the excised bands.

Table 1Identification of differentially produced proteins in *V. dahliae* Vd07038 both under nitrogen starvation and normal condition.

No.	Protein description	Band	ID	Score ¹	Score ²	ThMr (Da)	Thpl	Gravy	SignalP 4.1	TMHMM 2.0	SecretomeP 2.0	TatP 1.0
<i>Induced proteins (76)</i>												
<i>Cell wall degradation proteins (8)</i>												
1	Laccase-1	4	00034	30.28	–	60,928.7	8.63	–0.373	+		+	
2	Glucoamylase ^b	4	00408	40.25	40.25	67,311.0	4.81	–0.241	+		+	
3	Glucan 1,3-β-glucosidase	4	00511	20.24	–	50,402.0	4.01	–0.159	+		+	+
4	Ser/Thr protein phosphatase family protein ^b	4	02693	20.24	–	68,454.8	5.36	–0.398	+			
5	Pectinesterase	2, 6	07881	60.24	–	35,190.3	8.45	–0.214	+		+	+
6	Concanamycin induced protein C	–	09386	–	50.28	15,209.2	5.25	–1.586			+	
7	Unidentified transcript 2 ^b	1, 4	09675	30.26	–	50,978.8	4.46	–0.434	+		+	+
8	Glucan 1,3-β- glucosidase		09744	70.25	–	85,580.6	4.90	–0.187	+		+	+
<i>ROS scavenging and stress response proteins (9)</i>												
9	Cytochrome c peroxidase ^b	2	03116	60.20	–	40,289.3	7.70	–0.480			+	+
10	Mn superoxide dismutase ^b	4	07230	40.19	40.19	22,686.5	6.11	–0.228			+	
11	Hsp stress-seventy subfamily c1 ^b	4	00442	40.19	40.19	70,775.9	5.83	–0.399				+
12	Stress-induced protein 35 ^b	6, 8	01137	50.20	60.20	33,659.6	5.44	0.088				+
13	Disulfide-isomerase ^b	4	03047	60.29	60.29	55,023.9	4.66	–0.276	+			
14	Cap20 ^b	2	04049	50.19	–	20,309.8	7.84	–0.370			+	
15	Glucose-regulated protein ^b	3	05516	40.16	–	72,655.8	4.89	–0.393	+	+		+
16	Hsp70 ^b	2	08898	70.20	70.20	61,700.5	5.98	–0.112				+
17	Retrograde regulation protein ^b		09969	20.17	20.18	70,945.3	8.31	–0.410				+
<i>Lipid effectors (4)</i>												
18	Phosphatidylglycerol/phosphatidylinositol transfer protein ^b	6	00559	20.21	–	19,285.2	4.73	0.034	+			
19	SnodProt1 ^b	5	01852	30.31	40.36	14,265.8	4.85	0.119	+			
20	Pathogen-related yeast protein 1 ^b	2	04828	20.24	–	21,785.8	9.57	–0.451	+		+	
21	SnodProt1 ^b	1, 7, 8	06199	30.40	–	14,411.2	8.96	–0.087	+		+	
<i>Protein metabolism proteins (16)</i>												
22	Amidohydrolase family protein ^b	2	02965	20.20	–	106,079.7	5.92	–0.157		+		
23	Ubiquitin	8	00364	30.17	–	15,644.1	9.65	–0.683			+	+
24	FK506(tacrolimus) binding protein 1B ^b	1, 8	00423	20.24	–	15,951.1	9.49	–0.376			+	+
25	Carboxypeptidase S1 ^b	4, 8	00500	60.24	60.25	51,489.8	5.18	–0.179	+		+	
26	Vacuolar protease A ^b	2, 5, 6, 9	00825	30.24	50.25	43,461.7	4.80	–0.211			+	
27	Aspartate aminotransferase	3	01258	20.19	–	45,974.4	9.10	–0.174				+
28	Nascent polypeptide-associated complex α subunit ^b	4	02506	30.18	–	22,352.5	4.56	–0.777			+	
29	Cerevisin ^b	3	02670	30.21	30.21	56,007.5	5.79	–0.286	+			+
30	Proteasome component Pup3	2	03131	20.17	–	24,374.2	6.13	0.040				+
31	Glutamyl-tRNA amidotransferase ^b	4	03581	40.28	–	67,763.5	5.90	–0.001	+		+	+
32	Glutamine synthetase ^b	5	05884	20.23	–	39,941.8	5.73	–0.547			+	
33	Mitochondrial processing peptidase β subunit ^b	4	06877	30.16	–	53,026.3	5.66	–0.456				+
34	Serin endopeptidase ^b	3	08100	30.18	30.18	90,887.1	5.26	–0.188	+		+	
35	Elongation factor1-γ 1	2	08356	20.23	20.23	45,547.6	5.46	–0.409			+	
36	Glutamyl-tRNA amidotransferase subunit A ^b	1, 4	09944	30.22	–	49,953.0	5.65	–0.373			+	+
37	Glutamyl-tRNA amidotransferase subunit A ^b	8, 9	10386	20.20	–	43,883.7	4.92	–0.364			+	+
<i>Carbohydrate metabolism proteins (12)</i>												
38	Transketolase ^b	4	00251	50.26	50.26	74,803.5	5.57	–0.218				+
39	Isocitrate dehydrogenase subunit2	3	00455	20.19	–	41,008.4	8.51	0.021				+
40	NAD (P) H-dependent D-xylose reductase	3	01073	70.26	70.26	36,324.4	5.70	–0.157				+
41	Pyruvate dehydrogenase E1 component β subunit	3	01642	30.16	–	40,848.8	6.07	–0.018				+
42	Xylulose-5-phosphate phosphoketolase ^b	3, 5, 6, 9	02257	100.28	120.28	81,029.9	6.49	–0.394				+
43	Aconitate Hydratase ^b	3	02332	40.20	–	85,284.6	6.25	–0.333				+
44	Galactose-inducible crystalline-like yeast protein ^b	3	03683	70.24	70.24	36,531.4	5.87	–0.226			+	
45	Citrate synthase ^b	4	03946	30.19	40.17	51,835.1	7.68	–0.239				+
46	Malate dehydrogenase ^b	3, 4, 8	04607	60.22	–	28,310.6	4.79	–0.268			+	
47	Succinyl-CoA ligase α subunit ^b	3	04750	20.19	–	34,663.6	8.31	0.019				+
48	Ketol-acid reductoisomerase ^b	3	08589	30.17	–	44,944.7	8.59	–0.504				+
49	Dihydrolipoyl dehydrogenase ^b	4	09433	20.16	–	54,354.3	6.94	–0.144				+
<i>Electron-proton transport and energy metabolism proteins (11)</i>												
50	Cytochrome b-c1 ^b	6	00788	20.17	–	25,045.5	8.24	–0.252				+
51	NADH-cytochrome b5 reductase ^b	5	01016	20.14	–	36,325.5	9.22	–0.345			+	
52	Small COPII coat GTPase Sar1 ^b	2, 4	03565	30.23	–	21,623.0	6.05	–0.108	+			
53	Plasma membrane ATPase ^b	3	03948	30.17	60.19	96,230.3	4.98	0.110		+		
54	Cytochrome b-c1 complex subunit 2 ^b	4, 8	04054	80.34	–	47,560.8	9.17	–0.054				+
55	Inorganic pyrophosphatase ^b	3	04122	30.19	–	32,784.3	5.37	–0.497			+	
56	ATP synthase subunit 4	4	04250	30.21	–	26,407.2	9.01	–0.174				+
57	ATP-citrate synthase Subunit 1 ^b	3	06972	40.23	40.23	71,330.4	8.62	–0.065				+
58	ADP/ATP carrier protein ^b	2	07535	50.24	60.20	33,529.8	9.74	0.060		+	+	+
59	Oxidoreductase	3	07771	30.19	50.25	32,176.8	7.77	0.033				+
60	CHP, similar to FAD dependent oxidoreductase family protein from <i>Metarhizium anisopliae</i> ^b	2	09574	20.26	–	51,814.9	8.75	0.069	+		+	+

(continued on next page)

Table 1 (continued)

No.	Protein description	Band	ID	Score ¹	Score ²	ThMr (Da)	Thpl	Gravy	SignalP 4.1	TMHMM 2.0	SecretomeP 2.0	TatP 1.0
<i>Other functional proteins (16)</i>												
61	Tropomyosin ^b	1, 5, 6	01421	70.32	–	18,769.8	4.90	–1.221			+	
62	Adenylyl-sulfate kinase ^b	3	02995	20.21	–	23,503.4	5.89	–0.427				+
63	Guanyl-specific ribonuclease F1 complex Rieske subunit ^b	1	05416	40.26	30.20	13,078.6	9.51	–0.63	+		+	
64	Ribonuclease Trv ^b	3, 4	08888	60.34	–	39,097.6	5.70	–0.189	+		+	+
65	Cofilin	3	08897	20.25	–	16,965.0	5.32	–0.508			+	
66	1,3-β-glucanosyltransferase gel1 ^b	4	02243	30.30	40.30	49,399.6	4.67	–0.291	+		+	+
67	Secreted protein similar to hypothetical protein CH063_15848 from <i>Colletotrichum higginsianum</i> ^a	2, 8	04034	50.26	60.28	22,193.9	6.81	0.038	+	+	+	+
68	CHP, similar to hypothetical protein GLRG_03380 from <i>Colletotrichum graminicola</i> ^a	1, 3	00043	50.21	–	84,320.7	6.35	–0.762		+	+	
69	CHP, similar to transcription initiation factor <i>iia</i> small subunit from <i>Colletotrichum gloeosporioides</i> ^a	5	00544	20.23	–	24,892.1	4.93	–0.022		+	+	+
70	CHP, similar to cation transport protein from <i>Colletotrichum orbiculare</i> ^a	5	03251	20.19	–	24,374.4	4.65	–0.660			+	
71	CHP, similar to nonselective cation channel from <i>Colletotrichum fioriniae</i> ^a	3	03030	20.17	–	94,134.6	6.44	–0.007		+	+	+
72	CHP, similar to hypothetical protein UCREL1_5305 from <i>Eutypa lata</i> ^a	4	05713	20.20	–	41,392.8	8.09	0.223		+	+	
73	CHP, similar to hypothetical protein UCREL1_5305 from <i>Eutypa lata</i> ^a	2	05724	20.18	–	103,214.5	8.91	–0.763			+	
74	CHP, similar to hypothetical protein CH063_08994 from <i>Colletotrichum higginsianum</i> ^a	1	06225	60.23	70.23	38,368.8	4.73	–0.556			+	
75	Hypothetical protein, similar to immunogenic protein from <i>Colletotrichum orbiculare</i> ^a	8	06856	70.26	30.24	57,228.7	4.96	–0.554			+	+
76	CHP, similar to DNA replication regulator Sld3 from <i>Metarhizium robertsii</i> ^a	6	08779	20.18	–	101,116.7	9.68	–0.469			+	
<i>Suppressed proteins (9)</i>												
1	β-glucosidase ^b	3, 5	01263	120.28	–	66,556.9	6.28	–0.231			+	
2	Endo α-1,4 polygalactosaminidase precursor ^b	5	02829	30.34	–	32,764.7	8.67	–0.220	+			
3	Choline dehydrogenase	5	03639	20.24	–	68,888.4	5.18	–0.224	+			+
4	Secreted aspartic proteinase ^b	5	04979	30.17	–	62,898.3	5.59	–0.310	+	+	+	
5	Hypothetical protein, similar to hypothetical protein NECHADRAFT_123303 from <i>Nectria haematococca</i> ^a	6	05122	60.30	–	19,543.6	8.11	0.385	+			
6	Choline dehydrogenase ^b	–	08141	–	40.22	65,105.4	7.83	–0.073	+		+	
7	Endochitinase ^b	–	08741	–	80.24	73,177.6	6.37	–0.688	+		+	
8	Rhamnogalacturonase B	4	09063	40.19	40.19	57,158.4	6.42	–0.183	+		+	+
9	CHP, similar to hypothetical protein CFIO01_09475 from <i>Colletotrichum fioriniae</i> ^a	4	06511	20.26	–	52,291.5	9.30	–0.759			+	+
<i>Constitutively proteins (24)</i>												
1	Extracellular mutant33 ^b	4	00223	30.26	30.26	42,294.3	4.25	0.106	+			+
2	Outer mitochondrial membrane protein porin ^b	6	00272	50.17	50.17	29,729.4	9.14	–0.101			+	
3	Glucan 1,3-β-glucosidase ^b	3	02814	20.23	70.22	85,593.8	5.25	–0.102	+			
4	Peroxidase/catalase ^b	6, 8, 9	02834	90.21	100.27	83,560.0	5.69	–0.546			+	
5	Predicted protein, similar to hypothetical protein UCRPA7_3987 from <i>Togninia minima</i> ^a	6	0102	40.29	–	36,679.7	5.67	–0.514	+			
6	DJ-1/Pfpl family protein ^b	5	04348	40.20	50.23	27,893.4	5.02	0.021	+			+
7	Antigen1 ^b	1, 2, 3, 4, 5, 7, 8, 9	04551	50.28	120.26	26,743.7	4.92	–0.087	+			+
8	Hsp30 ^b	1, 3	04645	110.16	120.26	79,835.0	4.85	–0.579			+	
9	Tyrosinase ^b	2	04798	40.21	–	61,002.8	8.99	–0.345	+		+	+
10	Peroxidase/catalase ^b	3, 7, 8, 9	04826	100.24	280.26	84,331.7	5.89	–0.369	+		+	+
11	Lipase ^b	2, 6	05545	50.22	70.28	59,358.8	6.08	–0.086	+		+	+
12	Peptidyl-prolyl cis-trans isomerase ^b	2, 6, 7, 8	06261	60.27	–	19,650.9	7.84	–0.373			+	
13	Tripeptidyl-peptidase ^b	1, 2, 3, 5, 6, 7, 8, 9	06386	90.29	120.29	61,063.6	5.22	–0.191	+		+	+
14	Choline dehydrogenase	4	07266	20.14	60.26	65,414.5	6.81	–0.018	+			+
15	Glyceraldehyde 3-phosphate dehydrogenase ^b	5	08916	90.32	90.32	36,154.1	6.15	–0.102			+	
16	Isoamyl alcohol oxidase ^b	1, 2, 3, 4	09345	70.22	90.26	65,113.6	6.32	–0.182	+			+
17	Glucan 1,3-β-glucosidase	2, 3, 5	09510	100.28	100.28	51,252.3	5.38	–0.315	+		+	+
18	ATP synthase β subunit ^b	4	10013	100.26	110.27	55,268.9	5.24	–0.034			+	+
19	Ice nucleation protein ^b	3, 4, 5, 6, 7, 8, 9	10047	200.29	120.25	42,822.0	4.56	–0.474	+		+	
20	ATP synthase α subunit ^b	3	10347	80.24	90.24	59,828.5	9.15	–0.159				+
21	CHP, similar to hypothetical protein CGLO_04422 from <i>Colletotrichum gloeosporioides</i> ^a	5	00084	20.19	–	37,231.3	6.06	–0.013		+	+	
22	CHP, similar to hypothetical protein CGGC5_5484 from <i>Colletotrichum gloeosporioides</i> ^a	2, 3	00965	30.23	–	41,890.7	5.36	–0.480			+	
23	CHP, similar to extracellular serine-rich protein, putative from <i>Metarhizium acridum</i> ^a	2	08037	50.21	–	78,625.4	5.63	–0.258	+		+	+
24	CHP, similar to hypothetical protein CGLO_03430 from <i>Colletotrichum gloeosporioides</i> ^a	5	08827	30.23	20.23	78,796.0	9.69	–1.252			+	

gels were integrated together as another piece (Fig. 1). Then 9 gel pieces were washed with 50 mM NH_4HCO_3 and destained with 2 g/L potassium ferricyanide ($\text{K}_3\text{Fe}(\text{CN})_6$), 0.2 g/L sodium thiosulfate and ddH_2O for 15 min, respectively. After that, gel pieces were reduced with 10 mM dithiothreitol (DTT) and incubated at 50 °C for 15 min, followed by alkylation with 30 mM iodoacetamide (IAM) and incubated at room temperature in the dark for 15 min. The gel pieces were then washed with 50 mM NH_4HCO_3 and dried by the speed vacuum centrifugation for 10 min. Trypsin was added to the dry gel pieces at 37 °C for 16–18 h. Tryptic peptides were extracted with 60% ACN (acetonitrile), 5% TFA (trifluoroacetic acid) and 100% ACN. After the combined solution was dried, the pellet was resuspended in 0.1% formic acid and stored at -80 °C before mass spectrometry analysis. In the in-solution digestion, pellets of total dry biomass were dissolved with 50 mM Tris–HCl, pH 7.0 and washed with 50 mM NH_4HCO_3 . The following steps were the same as the in-gel digestion.

2.4. Liquid chromatography–nano-electrospray ionization tandem mass spectrometry (LC–nanoESI–MS) and protein identification

Tryptic peptides extracted from each gel band were analyzed by a Thermo LTQ linear ion trap mass spectrometry (Thermo Electron, San Jose, CA). Peptides were separated on-line by a fused silica capillary column packed with C18 resin (Jupiter 5 μm , 300 Å, Phenomenex, USA) using a linear gradient of 0.1% (v/v) formic acid in water (solvent A) and 4–60% acetonitrile (solvent B) over 50 min. Mass spectra were acquired in a survey scan from 400 to 2000 amu followed by five data-dependent MS–MS scans. All MS/MS data were searched against the National Center for Biotechnology Information (NCBI) non-redundant database by Bioworks version 3.2 software (SEQUEST, Thermo Electron) installed on a local server. Two missed trypsin cleavages were allowed with a static modification of +57 Da on cysteine residue. The precursor ion mass tolerance was 2.0 amu and the fragment ion mass tolerance was 1.0 amu. SEQUEST filter criteria were used as follows: (Xcorr \geq 1.9, 2.5 and 3.75 for +1, +2, and +3 charged peptides respectively, $\Delta\text{Cn} \geq$ 0.1, Rsp = 1). Each peptide assignment was also manually checked. Only proteins identified by two or more unique trypsin peptide matches were considered as confident hits. All these replicate biological samples were analyzed independently by LS–MS/MS analyses. Both significant hits (as defined by SEQUEST probability analysis) and hits that exceeded the arbitrarily set acceptance threshold (a peptide ion matching score of more than 20) were regarded as positive identifications.

2.5. Protein annotation and gene ontology (GO) category

Protein sequences were input to the InterPro member databases using the InterProScan Sequence Search server (<http://www.ebi.ac.uk/Tools/pfa/iprscan/>) to identify signatures. The compiled text outputs were subjected to GO categories using the Web Gene Ontology Annotation Plot (WEGO). Three groups of dataset were subjected to online analysis (<http://wego.genomics.org.cn/cgi-bin/wego/index.pl>).

2.6. Quantitative real-time PCR

RNA samples were extracted from the fungi with the total RNA Kit (Omega, USA). The cDNA was synthesized with the PrimeScript 1st

Strand cDNA Synthesis Kit (Takara, Japan). The transcription profiles of four genes that encode Snodprot1, glucan 1,3- β -glucosidases, glucoamylase P and Cipc, were analyzed by semi-quantitative RT-PCR and real-time PCR (Applied Biosystem, USA), respectively. Ubiquitin was selected as the house-keeping control. The primer sequences were listed in Table 2. The real-time PCR data were processed with $2^{-\Delta\Delta\text{CT}}$ [22].

3. Results and discussion

3.1. The growth of *V. dahliae* isolates under nitrogen starvation

In this study, biomass was measured to detect the growth and development state of *V. dahliae* isolates in Czapek–Dox broth (CDB) liquid medium with or without additional nitrogen source, respectively. Under the normal condition, the fungal dry weight was gradually increased and reached the maximum (stable phase) in 7–8 days, implying its highest bioactivity (Fig. 1A). After incubation for seven days under normal condition, the cells were transferred to the nitrogen starvation medium (CDB liquid medium without nitrogen) or fresh normal medium (as control), and further incubated for 5 days. As shown in Fig. 1B, the dry weight of *V. dahliae* grown under the nitrogen starvation medium showed a drastic decrease in the first 12 h, compared to that under the normal condition, indicating that the fungi are sensitive to the nitrogen starvation. We proposed that the nitrogen starvation might induce the signals for cell autolysis during the adjusting stage. However, the fungus adapts to this nitrogen depletion stress after 48 h as we can see a light increase of biomass from 48 to 72 h (Fig. 1B).

3.2. SDS-PAGE gradient gel and LC–MS analysis of secreted proteins

To further analyze the expression profile of secreted proteins of *V. dahliae* under nitrogen starvation condition, proteins in the supernatant were collected at different time points and separated by gradient SDS-PAGE. As seen from Fig. 1C and D, the amount of secreted proteins slowly increased and reached the maximum at 72 h. Thus, the protein bands after 72 h of nitrogen starvation were applied to LC–nano-ESI–MS–SEQUEST combined with BLAST search in the *V. dahliae* VdLs.17 genome database (http://www.broadinstitute.org/annotation/genome/verticillium_dahliae/MultiHome.html). There were totally 212 proteins identified, including 199 proteins from nitrogen starvation condition, compared to 50 proteins identified in the control (Fig. 2). These proteins were annotated based on the BLASTp analysis (Table 1).

3.3. Identification and physicochemical properties of the secreted proteins

A couple of bioinformatics analysis programs, including SignalP 4.1, SecretomeP 2.0, TatP 1.0 and TMHMM 2.0 [23–25], were used to predict secretome of *V. dahliae*. Although SignalP is the most commonly used program for predicting the signal peptide, it is not sufficient to assign all secreted proteins [26]. In addition, SecretomeP 2.0 and TatP 1.0 are two powerful programs to predict the atypical (or leaderless) secreted proteins, whereas TMHMM 2.0 has been used to predict the transmembrane helices in proteins [18]. Combination of these analyses enabled us to identify in total 109 secreted proteins, including 45 proteins with a signal peptide, 56 atypical secreted proteins and 8 outer-membrane proteins (Table 1).

Note to Table 1:

Proteins were classified according to their predicted functional categories.

Locus number in the *V. dahliae* VdLs.17 genome database from the Broad Institute.

(http://www.broadinstitute.org/annotation/genome/verticillium_dahliae/MultiHome.html).

¹ & ² indicated the protein which was identified by using in-gel and in-solution digestion, respectively.

The proteins listed here were all detected at least three times, and each score represents the highest of three independent replicates.

+ indicated the presence of putative sequence of SignalP 4.1, TMHMM 2.0, SecretomeP 2.0 or TatP 1.0.

Abbreviations: ID, locus number; ThMr, theoretical molecular weight; Thpl, theoretical isoelectric point; CHP, conserved hypothetical protein.

^a Indicated the protein firstly identified here.

^b Indicated the protein which firstly identified in *V. dahlia*, while has previously been reported in other organism.

Table 2
Primers used in this study.

Gene name	Gene ID	Forward (5' – 3')	Reverse (5' – 3')
Snodprot1	VDAG_01852	GCCGAACGTGCGGTACTCTGCT	ACCGCCTGTCCATTTCGTGAG
Glucosylase P	VDAG_00408	ACCGACCTCCCTACTAC	GCGAAGGTAGTCACGAATG
Glucan 1,3-β-glucosidases	VDAG_00511	TCTACCACCTCACCCACG	AAGCACTACCAGGAGCAACC
Cipc	VDAG_09386	TTCCCTGGTCCGAGGTT	TCACGCGGTCGTACTGCT
Ubiquitin	VDAG_05595	GCTCACCGGTAAGACTATCACA	TTGGACTTCACATTGTCGATCGT

Afterward we analyzed the physicochemical properties of all 109 secreted proteins. Their molecular masses were ranged from approximately 15 to 101 kDa, 87.2% of which are at 25 to 75 kDa. The pI values were distributed in a range of pH 4.25–9.74, with 88.1% proteins in the range of 4.0 to 6.0 and 8.0 to 10.0. We also analyzed their gravity of hydrophobicity, which exhibited a range from –1.586 to 0.385, and the scope of –0.5 to 0.0 was 86.2% (Fig. 3).

To explore the functions of these secreted proteins, we analyzed their sequences with InterPro annotation and Gene Ontology (GO) categories [27]. The compiled text outputs were subjected to GO categories using the Web Gene Ontology Annotation Plot (WEGO) online database analysis tools [28]. Three groups of dataset were simultaneously subjected to online analysis (<http://wego.genomics.org.cn/cgi-bin/wego/index.pl>) and shown in Fig. 4. Analyses of putative functions revealed that they were involved in 9 GO terms of cellular component, 5 GO terms of molecular function and 16 GO terms of biological process. In the cellular component category, most proteins were mapped to cell, cell part and organelle related GO terms. In the molecular function category, proteins were addressed to binding, catalytic activity and transporter, especially hydrolase activities, oxidoreductase activities and transferase activities. In biological process category, most proteins were involved in cellular process, metabolic process, development process and multicellular organism process.

3.4. Functional category of secreted proteins under nitrogen starvation condition

Among 109 secreted proteins, 24 proteins seemed to be constitutively expressed since they were detected under both nitrogen starvation and normal conditions. In contrast, 85 proteins were responsive to the nitrogen starvation stress. While 76 secreted proteins were induced as they were only detected under nitrogen starvation condition, the remaining 9 were suppressed since they were only identified in the normal condition (Table 1 and Fig. 2).

Interestingly, our physiological experiment in vivo showed that the sterilized secreted portions under nitrogen starvation condition rather than the normal condition could effectively protect cotton from the invasion of *V. dahliae* (data not shown). The secreted proteins specifically induced by nitrogen starvation stress were speculated to trigger the cellular immune response of the host plant to fight against the invasion of *V. dahliae*. Therefore, the 76 proteins induced by nitrogen starvation were subject to further analyses. On the basis of the predicted physiological functions and GO terms (Table 1), they were categorized into seven groups (Fig. 5): cell wall degrading (10.5%), reactive oxygen species (ROS) scavenging and stress response (11.8%), lipid effectors (5.3%), protein metabolism (21.1%), carbohydrate metabolism (15.8%), electron–proton transport and energy metabolism (14.5%), and other functional proteins (21.0%). The putative molecular functions and relations to the development and pathogenicity of *V. dahliae* will be discussed afterward.

3.4.1. Cell wall degrading related proteins

The phytopathogens should break through plant cell wall, the primary natural barrier, before successfully invading into the host plant. An effective strategy for fungi to overcome this barrier is to secrete a series of enzymes to break down the plant cell wall.

When fungi attack the plant, they generally utilize the nutrient source from plant cell wall, especially the degradation products of plant cell wall, such as pectin, which is one of core components of the cell wall [29]. For example, the fungi express cell wall degradation enzymes (CWDEs), such as glycosyl hydrolase, pectinesterase and laccase, to preferentially degrade polysaccharide, pectin and lignin. Upon these combined actions, the plant cell wall becomes less compact and more permeable. In consequence, more cell wall components will be exposed for the digestion by other enzymes, such as cellulase and hemicellulase [29,30].

On the basis of GO terms classification, eight induced proteins were predicted to involve in the degradation of the host cell wall. They are glucoamylase P, pectinesterase, laccase-1, Ser/Thr protein phosphatase family protein, concanamycin-induced protein C (Cipc), unidentified transcript 2 (Utr2) protein and two glucan 1,3-β-glucosidases. The glucoamylase P (*EC 3.2.1.20*) is to hydrolyze the terminal non-reducing α-(1,4)-linked D-glucose residues with release of α-D-glucose. Glucan 1,3-β-glucosidase (*EC 3.2.1.58*) is to hydrolyze the α-(1,6)-D-glucosidic linkages in some oligosaccharides produced from starch and glycogen. Pectinesterase (*EC 3.1.1.11*), also named pectin methylesterase, catalyzes the demethylesterification of cell wall pectin and releases the acidic pectate and methanol. Utr2 is homologous to the members from glycosyl hydrolase family 16 and may function in cell wall degradation. In addition, pectinesterase has also been reported to affect the pH of the cellular environment [31], in which way to increase cell wall porosity and cause swelling [32]. Proteins belonging to the Ser/Thr protein phosphatase family is similar to calcineurin-like phosphoesterase (*EC 3.1.-.-*) from *Colletotrichum graminicola* and was reported to mediate the cell growth and signaling [33]. Laccase (*EC 1.10.3.2*) is involved in lignin degradation, as well as in several other functions, such as sporulation, pathogenicity and detoxification [34]. Cipc, it has been found to be a cytoplasmic CWDE in several other fungi and might be secreted via a non-classical route to degrade host cell wall [35]. In addition, it was characterized to be an antibiotic resistance signal molecule [36–38]. To sum up, CWDEs can supply the energy and building blocks for the growth of pathogenic fungus through degrading plant cell wall. Furthermore, the expression of CWDEs was found to be induced when fungus was grown under nutrient stress conditions including nitrogen starvation during early fungal infection [39,40], because of the effective uptake of nutrient. Besides, CWDEs are also involved in cell wall soaking during plant infection [1], and their expression level can enhance the fungal pathogen virulence [41–44]. Therefore, we confirmed that these CWDEs induced by nitrogen starvation are involved in potential pathogenicity during early infection.

3.4.2. ROS scavenging and stress response related proteins

At the early stage of the fungal infection, host will respond to produce a quantity of ROS, which alters the redox status of the host cell, leading to hypersensitive responses and a hostile environment for pathogens [45,46]. To attack the host, the fungi secrete ROS scavenging proteins to neutralize or degrade ROS, making ROS ineffective.

Our results showed that two ROS scavenging proteins were induced in *V. dahliae* under the nitrogen starvation stress. They were manganese-superoxide dismutase (Mn-SOD, *EC 1.15.1.1*) and cytochrome c peroxidase (*EC 1.11.1.5*). Their functions in nitrogen starvation are detoxification of H₂O₂ to H₂O by oxidation of their different specific substrates. Hence,

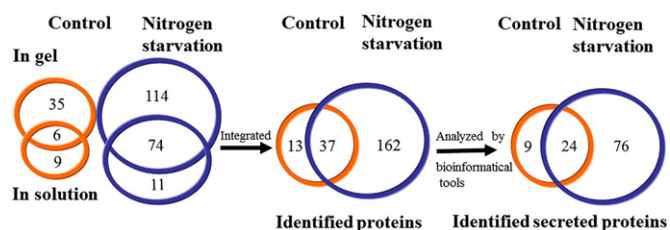


Fig. 2. Venn diagram showing the identification process of secreted proteins of *V. dahliae* under nitrogen starvation and control condition, respectively.

these ROS scavenging proteins may play a role in overcoming ROS stress and maintaining survival of *V. dahliae* in host.

Furthermore, stress-induced protein 35 (Sti35), stress-seventy subfamily c1 (Ssc1), pathogenesis associated protein Cap20, retrograde regulation protein, 78 kDa glucose-regulated protein, protein disulfide isomerase and heat shock protein 70 (Hsp70) were identified as stress sensors. Sti35 was identified as a bifunctional protein involved in oxidative stress response and thiamine biosynthesis in *Fusarium oxysporum* [47]. Ssc1 was regarded as an ATP-binding protein required for both import and folding of mitochondrial proteins in response to stress [48]. Retrograde regulation protein, the homologue Rtg2 in yeast, was found to be the sensor of mitochondrial dysfunction and its transcription is induced by the nitrogen starvation condition [49]. Protein disulfide isomerase (EC 5.3.4.1) was reported to be related to pathogen attachment–internalization and the regulation of ROS production by redox switches [50]. Therefore, these proteins in response to stress are benefit for governing the pathogen development when *V. dahliae* attacks the host plant.

3.4.3. Lipid effectors

Four proteins were identified as lipid effectors or potential allergen molecules of *V. dahliae*. Two are SnodProt1 like proteins, whereas the other two are phosphatidylglycerol/phosphatidylinositol transfer protein (PG/PITP) and pathogen-related yeast protein (Pry1).

SnodProt1 was firstly identified from the phytotoxic wheat pathogen *Stagonospora nodorum*. Here, we identified two SnodProt1 like proteins, VDAG_01852 and VDAG_06199, which share 84% sequence similarity, belong to the cerato-platanin family (pfam07249). The subsequent analysis (Fig. 6) showed that SnodProt1 (VDAG_01852) displays sequence similarity of 80, 78, 73, 71, 70, 67 and 67% to the eliciting plant response-like protein 1 (Epl1) from *Trichoderma asperellum* [51], small protein 1 (Sm1) from *Trichoderma virens* [52], protein related to plant expansions

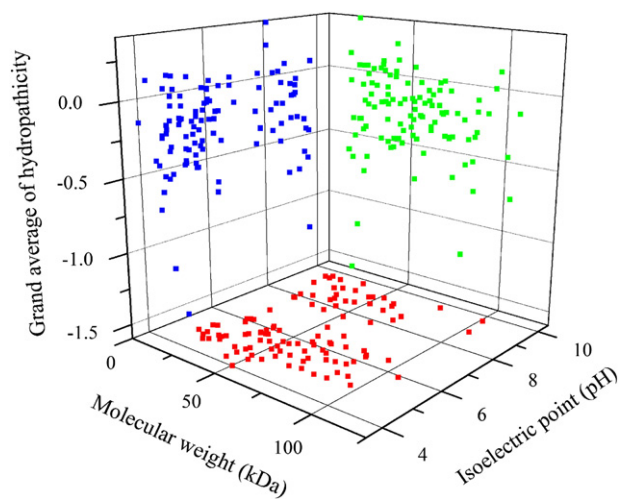


Fig. 3. The three-dimensional diagram of the secreted proteins of *V. dahliae*. The molecular weight (MW), isoelectric point (pI) and the grand average of hydropathicity values (GRAVY) of the identified proteins are shown as the three dimensions.

(Prpe) from *Botryotinia fuckeliana*, immunomodulatory protein (Immdp) from *Antrodia camphorata* [53], AspF13-like protein from *Curvularia lunata*, secreted protein 1 (Sp1) from *Leptosphaeria maculans* and heat-stable 19 kDa antigen from *Uncinocarpus reesii*, respectively. All these effectors contain four conserved cysteine residues and were classified into small cysteine rich proteins (SCRs). SCR with an even number of cysteine residues that form disulfide bridges were thought to function as effectors in the apoplast [54]. For example, Epl1 transcript was specifically detected under nitrogen starvation, involving in plant pathogenesis and elicitation of plant defense responses [51]. Sm1 can trigger the production of ROS and induce the expression of defense-related genes in cotton; and moreover, its expression is inducible throughout fungal development under nitrogen starvation. Moreover, pretreatment of cotton cotyledons with Sm1 provided high levels of protection to the foliar pathogen *T. virens* [52]. Immdp was characterized as a new immune-regulating agent from Taiwan fungus mycelium extract [53].

Another lipid effector PG/PITP belongs to the myeloid differentiation (MD)-2-related lipid recognition domain (ML domain) superfamily, involving in lipid recognition, phospholipids' transferring and recognition of pathogen related products and innate immunity [55]. Pry1 was also identified as the lipid effector, since it was the sterol-binding proteins related to the plant pathogen [56].

For the first time in *V. dahliae* we identified SnodProt1, PG/PITP and Pry1, the homologs of which are all important pathogenesis factors in other species. It is well known that the potential pathogenesis-associated proteins may help design target-directed fungicides for disease control. But further physiological experiments are required to approve whether they could really serve as candidate fungicides for controlling verticillium wilt disease.

3.4.4. Protein metabolism related proteins

Sixteen induced proteins involving in nitrogen metabolism, protein degrading and synthesis were identified under nitrogen starvation. Two proteases (vacuolar protease A and proteasome component Pup3), five peptidases (carboxypeptidase S1, serin endopeptidase, mitochondrial-processing peptidase β subunit, amidohydrolase family protein, cerevisin) are involved in fungal growth and development. Besides, the vacuolar proteinase was reported to play a major role in the activation of cellular proteases and initiate an activation cascade in *Saccharomyces cerevisiae* [57]; mutation of vacuolar protease Spm1 from the rice blast fungus *M. oryzae* was testified to cause the depression of fungal pathogenicity [58]. Carboxypeptidase was reported to be inducible during nitrogen deprivation [59]. Cerevisin, its homologous protein Kex2, was one of the virulence factors in the pathogenic fungi *Candida albicans* [60].

Glutamine synthetase, aspartate aminotransferase, glutamyl-tRNA amidotransferase, elongation factor1- γ 1, nascent polypeptide-associated complex α subunit, FK506 (tacrolimus) binding protein 1B and ubiquitin are involved in biosynthesis of different amino acids, protein synthesis and post-translational modification. Increased abundance of glutamine synthetase indicated that assimilation of nitrogen and biosynthesis of glutamine prevails when nitrogen source was lacking. Similar results were reported during pathogenesis of *Colletotrichum gloeosporioides* on host *Stylosanthes guianensis* [10]. Aspartate aminotransferase (EC 2.6.1.1) had been demonstrated to be essential for the phage infection by forming a complex with virus capsid protein [61]. Therefore, the increased expression of proteins related to amino acid metabolism, protein degradation and synthesis upon nitrogen starvation indicated that they might play important roles in the pathogenicity at fungal early infection.

3.4.5. Carbohydrate metabolism related proteins

Twelve proteins related to the carbohydrate metabolic process were identified, suggesting that nitrogen deprivation may change the carbohydrate metabolism level. Transketolase is involved in the fungal pentose phosphate pathway. Pyruvate dehydrogenase E1 component β subunit, dihydrolipoyl dehydrogenase, aconitate hydratase, isocitrate

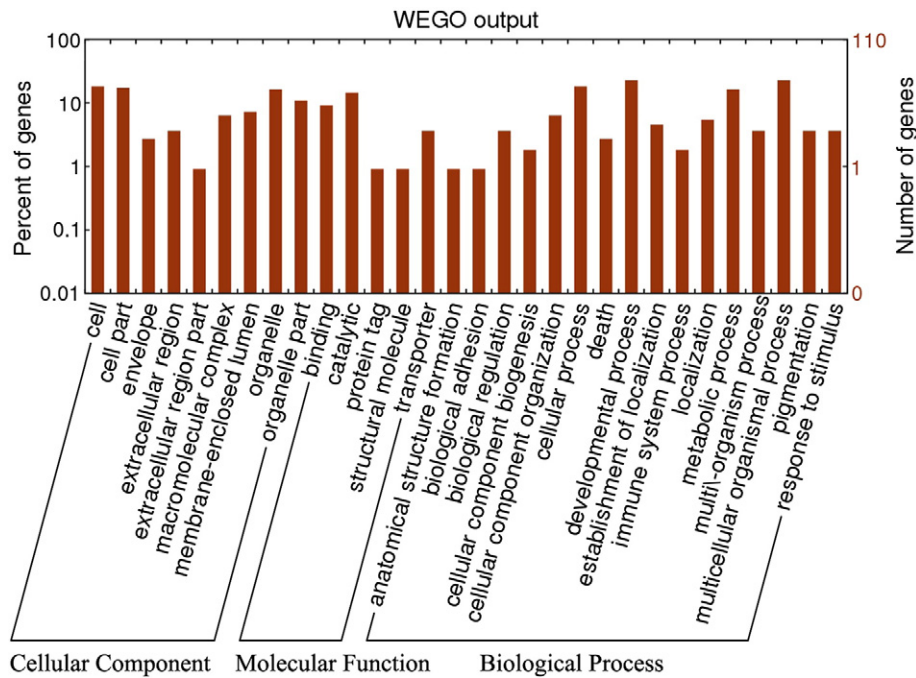


Fig. 4. The Web Gene Ontology Annotation Plot (WEGO) online database analysis outputs of the secreted proteins of *V. dahliae* (<http://wego.genomics.org.cn/cgi-bin/wego/index.pl>).

dehydrogenase subunit 2, xylulose-5-phosphate phosphoketolase, citrate synthase, and succinyl-CoA ligase α subunit are all involved in the pyruvate oxidation and citric acid cycle which could release quantities of energy. Galactose-inducible crystalline-like yeast protein, NADP(H)-dependent D-xylose reductase, malate dehydrogenase, and ketol-acid reductoisomerase all belong to the NAD/NADPH-dependent reductase and participate in carbohydrate metabolism. Meanwhile, they also contribute to ROS scavenging for producing NAD(P)H as an ultimate electron donor.

Moreover, malate dehydrogenase catalyzes the reversible conversion of oxalacetate and malate, whereas oxalacetate is an oxalic acid precursor and a pathogenicity factor in *B. cinerea* [62]. Malate dehydrogenase from *Colletotrichum acutatum* was also reported to involve the ROS scavenger, which was up-regulated both at the appressorium formation stage and under nitrogen-limiting condition [63]. Citrate synthase from *Agrobacterium* was confirmed to a virulence factor through its mutant assay [64]. Ketol-acid reductoisomerase from *Phytophthora infestans* was reported to be up-regulated in germinating cysts developing appressoria during the early, biotrophic phase [65]. Pyruvate dehydrogenase E1 component β subunit from *Lactobacillus plantarum* was proposed to assist the pathogen in adhesion to host tissues [66].

Taken together, the induced proteins related to intracellular carbohydrate metabolism can provide more energy for the growth of *V. dahliae*, and also probably affect the fungal pathogenicity under nitrogen starvation during the early invasion.

3.4.6. Electron-proton transport and energy metabolism related proteins

Eleven proteins detected under nitrogen starvation appear to be involved in electron-proton transport and energy metabolism. Among them, Oxidoreductase, cytochrome b-c1, NADH-cytochrome b5 reductase, and cytochrome b-c1 complex subunit 2, belong to the electron-proton transport system. These secreted mitochondrial proteins indicated the possibility of mitophagy upon nitrogen starvation, as reported previously [67]. Small COPII coat GTPase Sar1, Plasma membrane ATPase, ATP synthase subunit 4, inorganic pyrophosphatase, ATP-citrate synthase subunit 1, ADP/ATP carrier protein and conserved hypothetical protein 9574 are related to the ATP synthesis and degradation. Apart from these known functions, small COPII coat GTPase Sar1 (*EC* 3.6.5.-) is required for endomembrane trafficking and was established to be related to the invasion process [68]. Plasma membrane ATPase (*EC* 3.6.3.6) was confirmed as a target for antifungal drug development [69]. ATP synthase (*EC* 3.6.1.14) from *Bartonella henselae* is involved in the invasion process

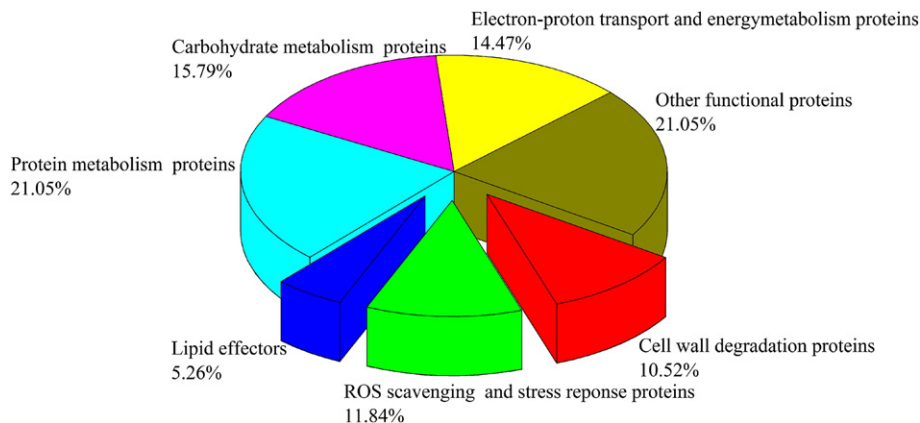


Fig. 5. Functional classification of the identified proteins that were induced under nitrogen starvation condition.

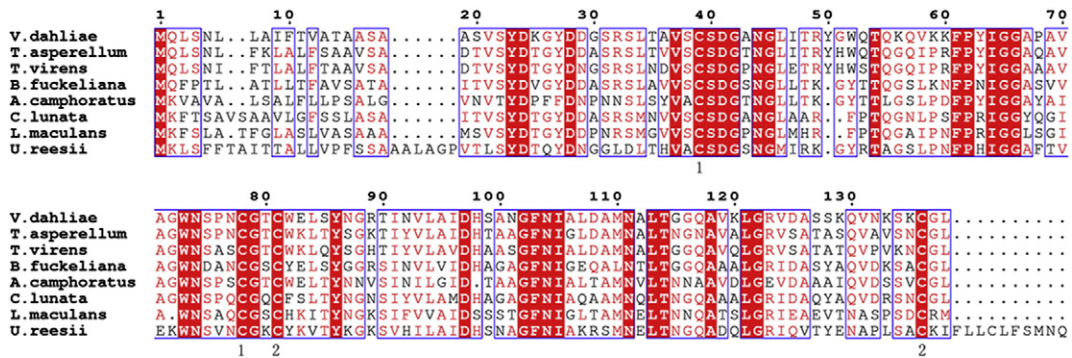


Fig. 6. Multiple-sequence alignment of Snodprot1 (VDAG_01852) and its homologs from other species of fungi. Identical residues were indicated in carmine. The alignment includes proteins known to be related to pathogenesis from phytopathogenic fungi: Eliciting plant response-like protein 1 (Epl1) from *Trichoderma asperellum* (similarity 80%); Extracellular small protein 1 (Sm1) from *T. vires* (similarity 78%); Protein related to plant expansions (Prpe) from *Botryotinia fuckeliana* (similarity 73%); Immunomodulatory protein (Immdp) from *Antrodia camphorata* (similarity 71%); Asp13-like protein from *Curvularia lunata* (similarity 70%); Secreted protein 1 (Sp1) from *Leptosphaeria maculans* (similarity 67%); Heat-stable 19 kDa antigen from *Uncinocarpus reesii* (similarity 67%). Numbers 1 and 2 indicate the positions of the cysteine residues participating in disulfide bonds.

[70]. The analysis implied that the energy metabolism related proteins not only offer the energy to maintain fungal growth, but also involve the pathogenesis of *V. dahliae* at the early invasion stage.

3.4.7. Other functional proteins

Tropomyosin and cofilin are related to the cytoskeleton/cell movement. Ribonuclease Trv and guanyl-specific ribonuclease F1 complex subunit Rieske are involved in nucleic acid metabolism. Adenylyl-sulfate kinase participates in purine metabolism and sulfur metabolism. 1,3-β-glucanosyltransferase gel1 may be a function in fungal cell wall degradation. Besides, eight proteins were annotated as conserved hypothetical protein (CHP) for their special characterized domain (Table 1), whereas two proteins, one secreted protein and one hypothetical protein, were identified with unknown function. Further investigation of function-unknown proteins could provide new insight into *V. dahliae* pathogenicity at the early infection stage.

3.5. Suppressed proteins under nitrogen starvation condition

Compared to the control, nine proteins could not be detected, indicating their decreased expression level under the nitrogen starvation condition; thus defined as suppressed proteins. Four proteins, β-glucosidase, endochitinase, rhamnogalacturonase B and endo α-1,4 polygalactosaminidase precursor, are related to the degradation of the cell wall. In addition, these include two choline dehydrogenases, an aspartic proteinase, a CHP and an HP. Most of these proteins are involved in the fungal cell wall remodeling; thus suppression of their expression might be related to the fungal growth retardation under nitrogen starvation.

3.6. Comparison of the secretome of *V. dahliae* with those of other fungi

To date, several secretomic studies on fungi have been carried out [12–17]. Here we identified for the first time in *V. dahliae* 72 secreted proteins such as SnodProt1, PG/PITP, Pry1, Sti35, Cap20, and Utr2. Moreover, we detected 17 novel proteins (Table 1 & Fig. 2), the biological functions of which need further investigations.

3.7. Expression profiles of the induced genes under nitrogen starvation

To further confirm the induced proteins under the nitrogen starvation condition, four representative genes that encode Snodprot1, glucan 1,3-β-glucosidase, glucoamylase P and Cipc were selected for the examination of transcriptional profiles with semi-quantitative RT-PCR and real-time PCR, respectively. As shown in Fig. 7, these four genes were all up-regulated under the nitrogen starvation, in consistence with the

results of LC–MS (Table 1). In details, genes coding for Snodprot1 and glucan 1,3-β-glucosidase were upregulated of about 1.5 and 2.8 folds, respectively, whereas genes encoding glucoamylase P and Cipc are induced to about 21.5 and 76.5 folds, respectively (Fig. 7B). These results indicated the high expression of genes that encode CWDEs, such as

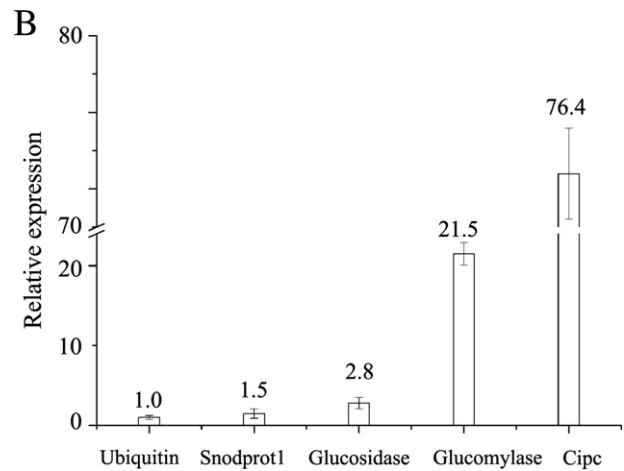
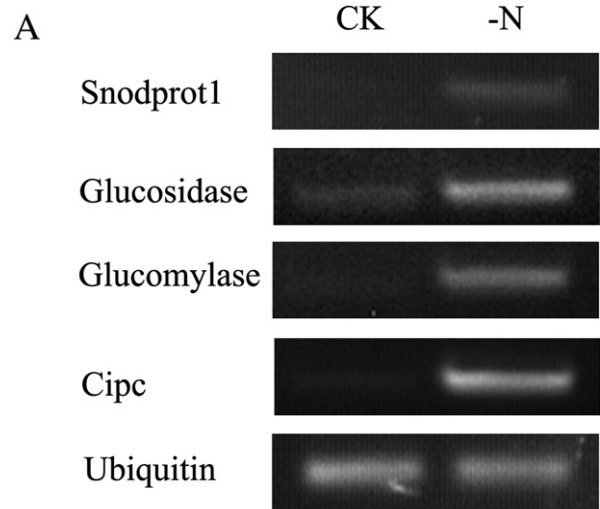


Fig. 7. (A) Semi-quantitative RT-PCR and (B) Real-time PCR. The transcription profiles of the four representative genes that encode Cipc, Snodprot1, Glucan 1,3-β-glucosidases and Glucoamylase P were shown. The results are means of three independent replicates (2^{-ΔΔCt}). Vertical bars indicate standard errors.

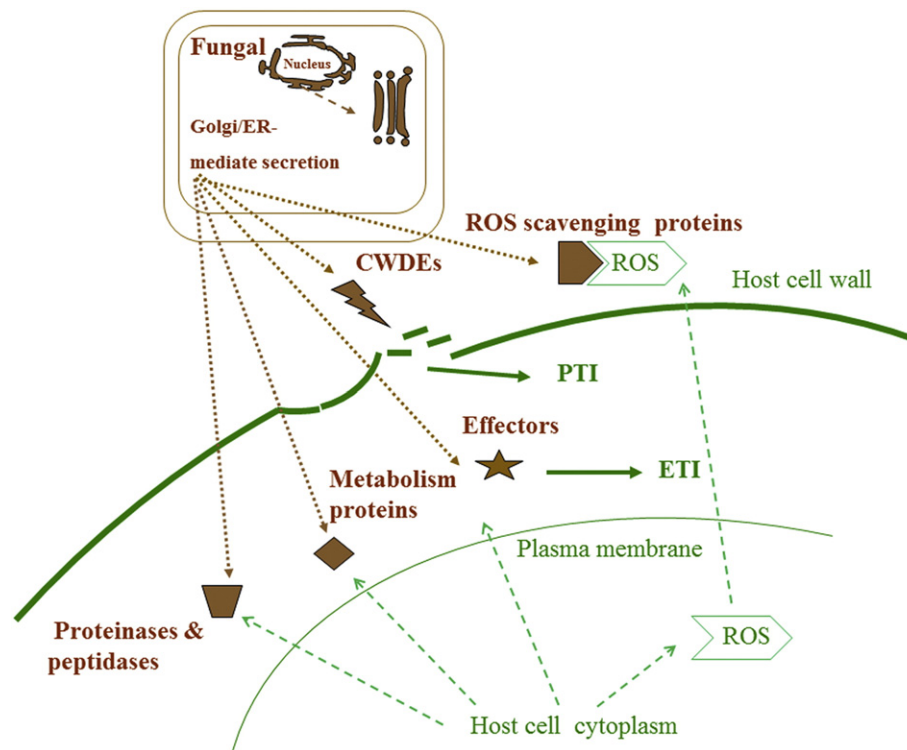


Fig. 8. A putative model of crosstalk between *V. dahliae* and host cell at the early stage of infection. The secreted proteins in response to nitrogen starvation are shown in brown. The reactions of host cell against *V. dahliae*'s invasion are shown in green. PTI and ETI stand for pathogen-associated molecular patterns and effector triggered immunity, respectively.

glucoamylase P, glucoamylase P and Cipc and lipid effectors Snodprot1 under nitrogen starvation.

3.8. A putative crosstalk between *V. dahliae* and host cell at the early stage of infection

The growth of fungi under nitrogen starvation condition was reported to mimic that at the early stage of infection to the plant cell [18]. Here we identified 76 proteins induced by nitrogen starvation, indicating that *V. dahliae* might secrete varieties of proteins at early infection process at the cost of its own nutrient utilization until a successful infection. Based on the present proteomics analysis, a putative crosstalk between *V. dahliae* and its host cell was hypothesized as shown in Fig. 8. That is, once the fungi *V. dahliae* encounter the host plant, they would secrete a variety of CWDEs to degrade and penetrate the plant cell wall. Afterwards, the host perceives the fungal invading probably by sensing the products of the CWDEs, and a cascade of signaling including pathogen-associated molecular patterns triggered immunity (PTI) are activated to protect the host plant from fungal attacks [71]. To survive in the host plant, the fungi secrete special ROS scavenging proteins to eliminate the ROS stress generally through NAD(P)H as reducing equivalents. At the same time, the fungal effector proteins and allergen signal molecules are expedited to initiate the effector triggered immunity (ETI) of the host cell to restrict the fungal development and virulence. In addition, the fungal metabolism is accelerated to gain more energy and nutrients, supporting further invasion and subsequent survival in the host cell.

4. Concluding remarks

Investigation of the secretome of phytopathogenic fungi will help us to understand the interaction between fungi and host plant. Here, we investigated the secretome of *V. dahliae* under nitrogen starvation condition, using in-gel and in-solution digestion combined with LC-nanoESI-MS. Though 1-D gel electrophoresis approach is of lower

resolution compared to 2-D gel electrophoresis, it is efficient to identify extreme proteins such as highly basic, acidic, or membrane proteins. A total of 212 proteins were identified; moreover the identification of 109 secreted proteins provides the first profile of the secretome of *V. dahliae* upon nitrogen starvation. Further investigations focusing on the molecular and cellular functions of these secreted proteins are needed for better understanding the molecular mechanism of verticillium wilt due to the infection of *V. dahliae*.

Transparency Document

The Transparency document associated with this article can be found, in the online version.

Acknowledgments

This study was supported by funds from the Ministry of Agriculture of China Project (2009ZX08009-37B). We also thank Ms. Gao Wu for the assistance of MS data analysis and Dr. Ying Xiong for technical advice.

Appendix A. Supplementary data

Supplementary data to this article can be found online at <http://dx.doi.org/10.1016/j.bbapap.2015.02.004>.

References

- [1] B.B.L., G.F. Pegg, *Verticillium Wilts*, CABI Publishing, New York, 2002, p. 432.
- [2] F. G.E., D. J.E., Differential effects of the defoliating and nondefoliating pathotypes of *Verticillium dahliae* upon the growth and development of *Gossypium hirsutum*, *Phytopathology* 72 (1982) 872–877.
- [3] E.F. Fradin, B.P. Thomma, Physiology and molecular aspects of *Verticillium* wilt diseases caused by *V. dahliae* and *V. albo-atrum*, *Mol. Plant Pathol.* 7 (2006) 71–86.
- [4] P.N. Dodds, G.J. Lawrence, A.M. Catanzariti, M.A. Ayliffe, J.G. Ellis, The *Melampsora lini* AvrL567 avirulence genes are expressed in haustoria and their products are recognized inside plant cells, *Plant Cell* 16 (2004) 755–768.

- [5] S.A. Hogenhout, R.A. Van der Hoorn, R. Terauchi, S. Kamoun, Emerging concepts in effector biology of plant-associated organisms, *Mol. Plant Microbe Interact.* 22 (2009) 115–122.
- [6] S. Snoeijs, A. Pérez-García, M.A.J. Joosten, P.G.M. De Wit, The effect of nitrogen on disease development and gene expression in bacterial and fungal plant pathogens, *Eur. J. Plant Pathol.* 106 (2000) 493–506.
- [7] N.J. Talbot, D.J. Ebbole, J.E. Hamer, Identification and characterization of MPG1, a gene involved in pathogenicity from the rice blast fungus *Magnaporthe grisea*, *Plant Cell* 5 (1993) 1575–1590.
- [8] M. Coleman, B. Henricot, J. Arnau, R.P. Oliver, Starvation-induced genes of the tomato pathogen *Cladosporium fulvum* are also induced during growth in planta, *Mol. Plant Microbe Interact.* 10 (1997) 1106–1109.
- [9] N.J. Talbot, H.R.K. McCafferty, M. Ma, K. Moore, J.E. Hamer, Nitrogen starvation of the rice blast fungus *Magnaporthe grisea* may act as an environmental cue for disease symptom expression, *Physiol. Mol. Plant Pathol.* 50 (1997) 179–195.
- [10] S.A. Stephenson, J.R. Green, J.M. Manners, D.J. Maclean, Cloning and characterisation of glutamine synthetase from *Colletotrichum gloeosporioides* and demonstration of elevated expression during pathogenesis on *Stylosanthes guianensis*, *Curr. Genet.* 31 (1997) 447–454.
- [11] N.M. Donofrio, Y. Oh, R. Lundy, H. Pan, D.E. Brown, J.S. Jeong, S. Coughlan, T.K. Mitchell, R.A. Dean, Global gene expression during nitrogen starvation in the rice blast fungus, *Magnaporthe grisea*, *Fungal Genet. Biol.* 43 (2006) 605–617.
- [12] B. Montanini, S. Gabella, S. Abba, M. Peter, A. Kohler, P. Bonfante, M. Chalot, F. Martin, S. Ottonello, Gene expression profiling of the nitrogen starvation stress response in the mycorrhizal ascomycete *Tuber borchii*, *Fungal Genet. Biol.* 43 (2006) 630–641.
- [13] V. Phalip, F. Delalande, C. Carapito, F. Goubet, D. Hatsch, E. Leize-Wagner, P. Dupree, A.V. Dorselaer, J.M. Jeltsch, Diversity of the exoproteome of *Fusarium graminearum* grown on plant cell wall, *Curr. Genet.* 48 (2005) 366–379.
- [14] O. Mueller, R. Kahmann, G. Aguilar, B. Trejo-Aguilar, A. Wu, R.P. de Vries, The secretome of the maize pathogen *Ustilago maydis*, *Fungal Genet. Biol.* 45 (Suppl. 1) (2008) S63–S70.
- [15] F.J. Fernández-Acero, T. Colby, A. Harzen, M. Carbú, U. Wieneke, J.M. Cantoral, J. Schmidt, 2-DE proteomic approach to the *Botrytis cinerea* secretome induced with different carbon sources and plant-based elicitors, *PROTEOMICS* 10 (2010) 2270–2280.
- [16] M.L. Medina, P.A. Haynes, L. Brecci, W.A. Francisco, Analysis of secreted proteins from *Aspergillus flavus*, *Proteomics* 5 (2005) 3153–3161.
- [17] X. Lu, J. Sun, M. Nimtz, J. Wissing, A.P. Zeng, U. Rinas, The intra- and extracellular proteome of *Aspergillus niger* growing on defined medium with xylose or maltose as carbon substrate, *Microb. Cell Fact.* 9 (2010) 23.
- [18] Y. Wang, J. Wu, Z.Y. Park, S.G. Kim, R. Rakwal, G.K. Agrawal, S.T. Kim, K.Y. Kang, Comparative secretome investigation of *Magnaporthe oryzae* proteins responsive to nitrogen starvation, *J. Proteome Res.* 10 (2011) 3136–3148.
- [19] A.F. El-Bebany, C. Rampitsch, F. Daayf, Proteomic analysis of the phytopathogenic soilborne fungus *Verticillium dahliae* reveals differential protein expression in isolates that differ in aggressiveness, *PROTEOMICS* 10 (2010) 289–303.
- [20] U.K. Laemmli, Cleavage of structural proteins during the assembly of the head of bacteriophage T4, *Nature* 227 (1970) 680–685.
- [21] R.C. Switzer Iii, C.R. Merrill, S. Shifrin, A highly sensitive silver stain for detecting proteins and peptides in polyacrylamide gels, *Anal. Biochem.* 98 (1979) 231–237.
- [22] A.L. Adam, G. Kohut, L. Hornok, Fphog1, a HOG-type MAP kinase gene, is involved in multistress response in *Fusarium proliferatum*, *J. Basic Microbiol.* 48 (2008) 151–159.
- [23] K. Hiller, A. Grote, M. Scheer, R. Munch, D. Jahn, PrediSi: prediction of signal peptides and their cleavage positions, *Nucleic Acids Res.* 32 (2004) W375–W379.
- [24] E.W. Klee, C.P. Sosa, Computational classification of classically secreted proteins, *Drug Discov. Today* 12 (2007) 234–240.
- [25] G. von Heijne, A new method for predicting signal sequence cleavage sites, *Nucleic Acids Res.* 14 (1986) 4683–4690.
- [26] M. Braaksma, E.S. Martens-Uzunova, P.J. Punt, P.J. Schaap, An inventory of the *Aspergillus niger* secretome by combining in silico predictions with shotgun proteomics data, *BMC Genomics* 11 (2010) 584.
- [27] E.M. Zdobnov, R. Apweiler, InterProScan – an integration platform for the signature-recognition methods in InterPro, *Bioinformatics* 17 (2001) 847–848.
- [28] J. Ye, L. Fang, H. Zheng, Y. Zhang, J. Chen, Z. Zhang, J. Wang, S. Li, R. Li, L. Bolund, J. Wang, WEGO: a web tool for plotting GO annotations, *Nucleic Acids Res.* 34 (2006) W293–W297.
- [29] V.E. Shevchik, M. Boccardo, R. Vedel, N. Hugouvieux-Cotte-Pattat, Processing of the pectate lyase PelI by extracellular proteases of *Erwinia chrysanthemi* 3937, *Mol. Microbiol.* 29 (1998) 1459–1469.
- [30] P. Reignault, O. Valette-Collet, M. Boccardo, The importance of fungal pectinolytic enzymes in plant invasion, host adaptability and symptom type, *Eur. J. Plant Pathol.* 120 (2008) 1–11.
- [31] J. Pelloux, C. Rusterucci, E.J. Mellerowicz, New insights into pectin methylesterase structure and function, *Trends Plant Sci.* 12 (2007) 267–277.
- [32] L. Taiz, E. Zeiger, Secondary metabolites and plant defense, *Plant Physiol.* 4 (2006) 315–344.
- [33] V. Janssens, J. Goris, Protein phosphatase 2A: a highly regulated family of serine/threonine phosphatases implicated in cell growth and signalling, *Biochem. J.* 353 (2001) 417–439.
- [34] C.F. Thurston, The structure and function of fungal laccases, *Microbiology* 140 (1994) 19–26.
- [35] B. Bauer, M. Schwienbacher, M. Broniszewska, L. Israel, J. Heesemann, F. Ebel, Characterisation of the CipC-like protein AFUA_5G09330 of the opportunistic human pathogenic mould *Aspergillus fumigatus*, *Mycoses* 53 (2010) 296–304.
- [36] P. Melin, J. Schruener, E.G. Wagner, Proteome analysis of *Aspergillus nidulans* reveals proteins associated with the response to the antibiotic concanamycin A, produced by Streptomycetes species, *Mol. Genet. Genomics* 267 (2002) 695–702.
- [37] K.C. Tan, J.L. Heazlewood, A.H. Millar, G. Thomson, R.P. Oliver, P.S. Solomon, A signaling-regulated, short-chain dehydrogenase of *Stagonospora nodorum* regulates asexual development, *Eukaryot. Cell* 7 (2008) 1916–1929.
- [38] R. Li, R. Rimmer, L. Buchwaldt, A.G. Sharpe, G. Seguin-Swartz, C. Coutu, D.D. Hegedus, Interaction of *Sclerotinia sclerotiorum* with a resistant *Brassica napus* cultivar: expressed sequence tag analysis identifies genes associated with fungal pathogenesis, *Fungal Genet. Biol.* 41 (2004) 735–753.
- [39] C. Larsson, U. von Stockar, I. Marison, L. Gustafsson, Growth and metabolism of *Saccharomyces cerevisiae* in chemostat cultures under carbon-, nitrogen-, or carbon- and nitrogen-limiting conditions, *J. Bacteriol.* 175 (1993) 4809–4816.
- [40] A. Abbas, H. Koc, F. Liu, M. Tien, Fungal degradation of wood: initial proteomic analysis of extracellular proteins of *Phanerochaete chrysosporium* grown on oak substrate, *Curr. Genet.* 47 (2005) 49–56.
- [41] A. Isshiki, K. Akimitsu, M. Yamamoto, H. Yamamoto, Endopolygalacturonase is essential for citrus black rot caused by *Alternaria citri* but not brown spot caused by *Alternaria alternata*, *Mol. Plant Microbe Interact.* 14 (2001) 749–757.
- [42] B. Oeser, P.M. Heidrich, U. Muller, P. Tudzynski, K.B. Tenberge, Polygalacturonase is a pathogenicity factor in the *Claviceps purpurea*/rye interaction, *Fungal Genet. Biol.* 36 (2002) 176–186.
- [43] C.A. Voigt, W. Schafer, S. Salomon, A secreted lipase of *Fusarium graminearum* is a virulence factor required for infection of cereals, *Plant J.* 42 (2005) 364–375.
- [44] N. Brito, J.J. Espino, C. Gonzalez, The endo-beta-1,4-xylanase xyn11A is required for virulence in *Botrytis cinerea*, *Mol. Plant Microbe Interact.* 19 (2006) 25–32.
- [45] A. Tanaka, M.J. Christensen, D. Takemoto, P. Park, B. Scott, Reactive oxygen species play a role in regulating a fungus-perennial ryegrass mutualistic interaction, *Plant Cell* 18 (2006) 1052–1066.
- [46] G. Qin, S. Tian, Z. Chan, B. Li, Crucial role of antioxidant proteins and hydrolytic enzymes in pathogenicity of *Penicillium expansum*: analysis based on proteomics approach, *Mol. Cell. Proteomics* 6 (2007) 425–438.
- [47] C. Ruiz-Roldan, L. Puerto-Galan, J. Roa, A. Castro, A. Di Pietro, M.I. Roncero, C. Hera, The *Fusarium oxysporum* sti35 gene functions in thiamine biosynthesis and oxidative stress response, *Fungal Genet. Biol.* 45 (2008) 6–16.
- [48] S. Schmidt, A. Strub, K. Rottgers, N. Zufall, W. Voos, The two mitochondrial heat shock proteins 70, Ssc1 and Ssq1, compete for the cochaperone Mge1, *J. Mol. Biol.* 313 (2001) 13–26.
- [49] A. Komeili, K.P. Wedaman, E.K. O'Shea, T. Powers, Mechanism of metabolic control. Target of rapamycin signaling links nitrogen quality to the activity of the Rtg1 and Rtg3 transcription factors, *J. Cell Biol.* 151 (2000) 863–878.
- [50] B.S. Stolf, I. Smyrniak, L.R. Lopes, A. Vendramin, H. Goto, F.R. Laurindo, A.M. Shah, C.X. Santos, Protein disulfide isomerase and host-pathogen interaction, *Sci. World J.* 11 (2011) 1749–1761.
- [51] V. Seidl, M. Marchetti, R. Schandl, G. Allmaier, C.P. Kubicek, Epl1, the major secreted protein of *Hypocrea atroviridis* on glucose, is a member of a strongly conserved protein family comprising plant defense response elicitors, *FEBS J.* 273 (2006) 4346–4359.
- [52] S. Djonovic, M.J. Pozo, L.J. Dangott, C.R. Howell, C.M. Kenerley, Sm1, a proteinaceous elicitor secreted by the biocontrol fungus *Trichoderma virens* induces plant defense responses and systemic resistance, *Mol. Plant Microbe Interact.* 19 (2006) 838–853.
- [53] F. Sheu, P.J. Chien, K.Y. Hsieh, K.L. Chin, W.T. Huang, C.Y. Tsao, Y.F. Chen, H.C. Cheng, H.H. Chang, Purification, cloning, and functional characterization of a novel immunomodulatory protein from *Antrodia camphorata* (bitter mushroom) that exhibits TLR2-dependent NF-kappaB activation and M1 polarization within murine macrophages, *J. Agric. Food Chem.* 57 (2009) 4130–4141.
- [54] S. Kamoun, A catalogue of the effector secretome of plant pathogenic oomycetes, *Annu. Rev. Phytopathol.* 44 (2006) 41–60.
- [55] N. Inohara, G. Nuñez, ML – a conserved domain involved in innate immunity and lipid metabolism, *Trends Biochem. Sci.* 27 (2002) 219–221.
- [56] V. Choudhary, R. Schreiber, Pathogen-Related Yeast (PRY) proteins and members of the CAP superfamily are secreted sterol-binding proteins, *Proc. Natl. Acad. Sci. U. S. A.* 109 (2012) 16882–16887.
- [57] N. Vazquez-Laslop, K. Tenney, B.J. Bowman, Characterization of a vacuolar protease in *Neurospora crassa* and the use of gene RIPing to generate protease-deficient strains, *J. Biol. Chem.* 271 (1996) 21944–21949.
- [58] H. Saitoh, S. Fujisawa, A. Ito, C. Mitsuoka, T. Berberich, Y. Tosa, M. Asakura, Y. Takano, R. Terauchi, SPM1 encoding a vacuole-localized protease is required for infection-related autophagy of the rice blast fungus *Magnaporthe oryzae*, *FEMS Microbiol. Lett.* 300 (2009) 115–121.
- [59] R.J. Stieger, M.J. Bidochka, D.W. Roberts, Characterization of a novel carboxypeptidase produced by the entomopathogenic fungus *Metarhizium anisopliae*, *Arch. Biochem. Biophys.* 314 (1994) 392–398.
- [60] G. Newport, A. Kuo, A. Flattery, C. Gill, J.J. Blake, M.B. Kurtz, G.K. Abruzzo, N. Agabian, Inactivation of Kex2p diminishes the virulence of *Candida albicans*, *J. Biol. Chem.* 278 (2003) 1713–1720.
- [61] Y. Chen, D. Wei, Y. Wang, X. Zhang, The role of interactions between bacterial chaperone, aspartate aminotransferase, and viral protein during virus infection in high temperature environment: the interactions between bacterium and virus proteins, *BMC Microbiol.* 13 (2013) 48.
- [62] R. Gonzalez-Fernandez, K. Aloria, J. Valero-Galvan, I. Redondo, J.M. Arizmendi, J.V. Jorriñ-Novo, Proteomic analysis of mycelium and secretome of different *Botrytis cinerea* wild-type strains, *J. Proteomics* 97 (2014) 195–221.
- [63] S.H. Brown, O. Yarden, N. Gollop, S. Chen, A. Zveibil, E. Belausov, S. Freeman, Differential protein expression in *Colletotrichum acutatum*: changes associated with reactive oxygen

- species and nitrogen starvation implicated in pathogenicity on strawberry, *Mol. Plant Pathol.* 9 (2008) 171–190.
- [64] M. Suksomtip, P. Liu, T. Anderson, S. Tungpradabkul, D.W. Wood, E.W. Nester, Citrate synthase mutants of *Agrobacterium* are attenuated in virulence and display reduced vir gene induction, *J. Bacteriol.* 187 (2005) 4844–4852.
- [65] L.J. Grenville-Briggs, A.O. Avrova, C.R. Bruce, A. Williams, S.C. Whisson, P.R. Birch, P. van West, Elevated amino acid biosynthesis in *Phytophthora infestans* during appressorium formation and potato infection, *Fungal Genet. Biol.* 42 (2005) 244–256.
- [66] V. Vastano, M. Salzillo, R.A. Siciliano, L. Muscariello, M. Sacco, R. Marasco, The E1 beta-subunit of pyruvate dehydrogenase is surface-expressed in *Lactobacillus plantarum* and binds fibronectin, *Microbiol. Res.* 169 (2014) 121–127.
- [67] A. Eiyama, N. Kondo-Okamoto, K. Okamoto, Mitochondrial degradation during starvation is selective and temporally distinct from bulk autophagy in yeast, *FEBS Lett.* 587 (2013) 1787–1792.
- [68] B. Cevher-Keskin, ARF1 and SAR1 GTPases in endomembrane trafficking in plants, *Int. J. Mol. Sci.* 14 (2013) 18181–18199.
- [69] P. Soteropoulos, T. Vaz, R. Santangelo, P. Paderu, D.Y. Huang, M.J. Tamas, D.S. Perlin, Molecular characterization of the plasma membrane H⁽⁺⁾-ATPase, an antifungal target in *Cryptococcus neoformans*, *Antimicrob. Agents Chemother.* 44 (2000) 2349–2355.
- [70] C.C. Chang, Y.J. Chen, C.S. Tseng, W.L. Lai, K.Y. Hsu, C.L. Chang, C.C. Lu, Y.M. Hsu, A comparative study of the interaction of *Bartonella henselae* strains with human endothelial cells, *Vet. Microbiol.* 149 (2011) 147–156.
- [71] A. Kombrink, A. Sánchez-Vallet, B.P.H.J. Thomma, The role of chitin detection in plant–pathogen interactions, *Microbes Infect.* 13 (2011) 1168–1176.